

## Nuclear topography of the 1q21 genomic region and Mcl-1 protein levels associated with pathophysiology of multiple myeloma

S. LEGARTOVA<sup>1</sup>, J. KREJCI<sup>1</sup>, A. HARNICAROVA<sup>1</sup>, R. HAJEK<sup>2</sup>, S. KOZUBEK<sup>1</sup>, E. BARTOVA<sup>1\*</sup>

<sup>1</sup> Institute of Biophysics, Academy of Sciences of the Czech Republic, Královopolská 135, 612 65 Brno, Czech Republic, e-mail: bartova@ibp.cz,

<sup>2</sup> Department of Internal Medicine-Hematology, Masaryk University Hospital, 625 00, Brno, Czech Republic

Received February 9, 2009

Chromosomal rearrangements and copy number variation are frequently observed in cancer cells, including multiple myeloma (MM). Karyotypic abnormalities seen in MM cells correlate with the disease stage and drug responses. Here, we investigate the nuclear arrangement of the 1q21 region; amplification of this region is an important diagnostic and prognostic marker of MM. We examined the lymphoblastoid cell line CD138<sup>+</sup> ARH-77, multiple myeloma CD138<sup>+</sup> MOLP-8 cells, and the CD138<sup>+</sup> bone marrow fraction of patients diagnosed with MM. In this experimental system, we observed that gamma-radiation and selected cytostatic drugs such as melphalan and dexamethasone did not significantly alter the nuclear radial arrangement of the 1q21 region and other relevant regions of chromosome 1. Similarly, conserved nuclear radial positioning after cytostatic treatment was observed for the *c-myc*, *TP53*, *CCND1*, and *IgH* loci. When analyzed Mcl-1, a protein encoded by a gene mapped to the 1q21 region, we found that the variant Mcl-1<sub>s</sub> is highly expressed in multiple myeloma MOLP-8 cells, but not in peripheral blood lymphocytes of healthy donors or lymphoblastoid ARH-77 cells; this is in contrast to the expression pattern of the Mcl-1<sub>L</sub> variant. On the basis of these observations we suggest that the 1q21 region is an important diagnostic marker of MM, particularly the gene encoding the Mcl-1<sub>s</sub> variant, which can be easily detected by western analysis.

*Key words: Multiple myeloma, 1q21, DNA-FISH*

Karyotypic instability is common in most tumor cells, including multiple myeloma (MM) [1, 2]. The presence of karyotypic abnormality, particularly hypodiploidy, correlates strongly with a poor prognosis in multiple myeloma [3]. Karyotype profiles of MM are very similar to those of some epithelial tumors and in the blast phase of chronic myelogenous leukemia [4]. Analyses using comparative genomic hybridization microarrays have revealed that gains and losses in specific chromosome arms are frequently observed in myeloma cell populations [5]. Deletion of the 13q region, which includes the retinoblastoma tumor suppressor gene, is a prominent cytogenetic marker of MM [6]. However, some patients in which the 13q14.3 region is retained show a gain at the 11q23 region. This distinct subgroup of MM is also associated with an unfavorable prognosis [7]. Fluorescence in situ hybridization (FISH) techniques have enabled the

identification of other cytogenetic markers, such as the gain of 1q21 and the translocation t(4;14) [5, 7], which have been relevant to clinical output. Translocations involving the *IgH* locus (14q32) are very common in MM. In addition to the t(4;14) translocation, *IgH* can also translocate to other regions, such as 11q13, 6p21, and 12p13, which encode cyclins D1, D2, and D3, respectively. A common secondary translocation involving *IgH* and the protooncogene *c-myc* (8q24.21) is detected in 15% of patients at all stages of multiple myeloma [8]. Mutations in other protooncogenes, such as *KRAS2* and *NRAS*, are also associated with poor prognosis [9]. In addition, the abnormal expression of only three genes, *RAN* (6p21), *ZHX-2* (8q24.3), and *CHC1L* (13q14.3) have been found to be correlated with rapid relapse [10]. Interestingly, each of these genes influences the prognosis independently, so that the combination of *RAN* over-expression and decreased expression of *ZHX-2* and *CHC1L* represents an unfavorable prognostic indicator [10].

In this study we explored the nuclear arrangement of the 1q21 region, which is one of the important chromosomal aber-

\* Corresponding author

rations in MM and even in other tumors, in myeloma cells [11, 12, 13, 14]. It has been shown that amplification of the 1q21 region is associated with poor prognosis [15]. Hanamura et al. [15] showed that 1q21 amplification is low in monoclonal gammopathy of undetermined significance (MGUS) and it increases to 43% in the transition of MGUS to MM and to 72% at relapse. This genetic alteration is closely associated with inappropriate regulation of expression of the *c-MAF* and *MMSET/FGFR3* genes. Moreover, 1q21 amplification is often associated with deletion at chromosome 13 involving the retinoblastoma tumor suppressor gene (*Rb1*), which is associated with a more aggressive clinical manifestation of the disease [16]. The presence of more than four copies of 1q21 is associated with resistance to available anticancer treatment; patients with amplification of 1q21 do not respond to thalidomide therapy [16]. The significance of 1q21 amplification in the progression of MM is not clear and efforts have been directed toward identifying the molecular mechanism underlying this genomic aberration. It can be shown that the *CKS1B*, *BCL-9*, or *RAB25* genes can be involved in 1q21 amplification [17] and the gene encoding p27KIP1, which is a cyclin-dependent kinase inhibitor, are considered to have a role in MM tumorigenesis [18]. Together, these observations demonstrate that 1q21 amplification is associated with unfavorable MM prognosis accompanied by the absence of a response to thalidomide treatment. Therefore, new cytostatic drugs should be evaluated for use in treatment of myeloma.

Here, we provide a detailed procedure for the preparation of DNA FISH probes for clinical studies on 1q21 amplification. We have analyzed the nuclear radial distribution and karyotypic stability of the 1q21 region in the MM cell line MOLP-8 (CD138<sup>+</sup>) and in the multiple myeloma-related, EBV<sup>+</sup> lymphoblastoid cell line ARH-77 (CD138<sup>-</sup>). The ARH-77 cell line has a karyotype and IgG level similar to CD 138<sup>+</sup> MM cell lines [19, 20]. We also investigated the effects of gamma-radiation and the cytostatic drugs melphalan and dexamethasone in these two cell lines. Karyotype changes were also examined in CD138<sup>+</sup> cells of patients diagnosed with MM. In an effort to identify a marker of MM that could potentially serve as a diagnostic tool, we explored the myeloid cell leukemia-1 protein (*Mcl-1*), which is encoded by a gene mapped to the 1q21 region. *Mcl-1* was originally identified as an antiapoptotic protein and has two alternatively spliced variants, *Mcl-1<sub>s</sub>* (32 kDa, short) and *Mcl-1<sub>L</sub>* (40 kDa, long) [21, 22]. We observed a remarkable feature of *Mcl-1* in MM cells. The *Mcl-1<sub>s</sub>* variant was expressed at a high level in MOLP-8 cells but was detected at only a very low level in the EBV<sup>+</sup> lymphoblastoid cell line ARH-77 by western analysis. The full-length variant *Mcl-1<sub>L</sub>* was expressed at a high level in both ARH-77 and MOLP-8 cells; however, expression of *Mcl-1<sub>L</sub>* in peripheral blood lymphocytes of healthy donors was quite low. On the basis of this observation we propose that *Mcl-1<sub>s</sub>* protein expression level could serve as a diagnostic marker of MM if validation in a large group of patients and demonstration of statistically significant results can be achieved.

## Materials and methods

*Cell lines, cytostatic treatments, and clinical samples.* Lymphoblastoid ARH-77 (CD138<sup>-</sup>) and multiple myeloma MOLP-8 (CD138<sup>+</sup>) cells (both from DSMZ, Braunschweig, Germany) were seeded at densities of  $2 \times 10^5$  and  $4 \times 10^5$  cells/ml, respectively, and cultured in RPMI-1640 medium supplemented with 10% and 20%, respectively, fetal calf serum (PAN, Germany), 100 IU/ml penicillin, and 0.1 mg/ml streptomycin at 37° C in a humidified atmosphere of 5% CO<sub>2</sub>/95% air. Twenty-four hours after plating, the cells were treated with melphalan (20 mM dissolved in ethanol), dexamethasone (5 mM dissolved in DMSO), or gamma-radiation (<sup>60</sup>Co) at a dose of 10 Gy. After treatment the cells were cultured for an additional 24 hours and harvested for FISH and western analysis.

Clinical samples of bone marrow cells and peripheral blood lymphocytes were obtained from the Department of Internal Medicine-Hematology, Masaryk University Hospital in Brno. The plasma cell CD138<sup>+</sup> MM fraction was prepared from bone marrow biopsies using a separator (VarioMACS, no.: 431-02) [23] and used in the analysis. Lymphocytes were isolated from peripheral blood of healthy donors by Ficoll-Hypaque gradient centrifugation as described by Bártová et al. [24] and used as controls.

*DNA probe preparation for fluorescence in situ hybridization (FISH).* DNA/DNA hybridization was carried out with probes prepared from clones from the BAC/PAC library of Prof. M. Rocchi (Bari, Italy). We used the two BAC clones, RP11-205M9 and RP11-42A2, which contain the 1q21 insert (see Fig. 1A for 1q21 region mapped on HSA1). BAC DNA was isolated by the standard anion-exchange procedure using a QIAGEN Large Construct Kit (QIAGEN, #12462). The purified DNA fragments were labeled using a DIG- or Biotin-Nick Translation Mix (Roche, Germany). In this procedure every twentieth to twenty-fifth nucleotide is modified with digoxigenin-11-dUTP or biotin-16-dUTP; the fragment length of the labeled DNA is 200 - 500 bp (Fig. 1B). For the nick translation reaction, 1 µg of DNA was dissolved in double-distilled water to a final volume of 16 µl followed by the addition of 4 µl DIG- or Biotin-Nick Translation Mix and incubation at 15°C for 90 min. The reaction was stopped by the addition of 1 µl 0.5M EDTA and heating at 65°C for 10 min. Following nick translation human Cot-1 DNA (Roche) was added to ensure effective suppression of cross-hybridization to repetitive elements. In this reaction, 120 ng of DIG- or biotin-labeled DNA, 6 µg of Cot-1 DNA, and salmon sperm DNA to a total amount of 20 µg DNA were combined followed by the addition of 1/10 volume 3M sodium acetate and 2 volumes pre-chilled 96% ethanol and incubation at 70°C for 30 min. The samples were then centrifuged at 13,500 rpm for 15 min and the pellet was washed with 400 µl 70% ethanol, which had been pre-cooled to -20°C. The pellet was lyophilized and dissolved in 20 µl hybridization buffer (Hybrizol VII, Oncor, USA). In preparation for fluorescence in situ hybridization (FISH) cells were washed twice in PBS, fixed in 3.7% formaldehyde, washed again in PBS, and treated with

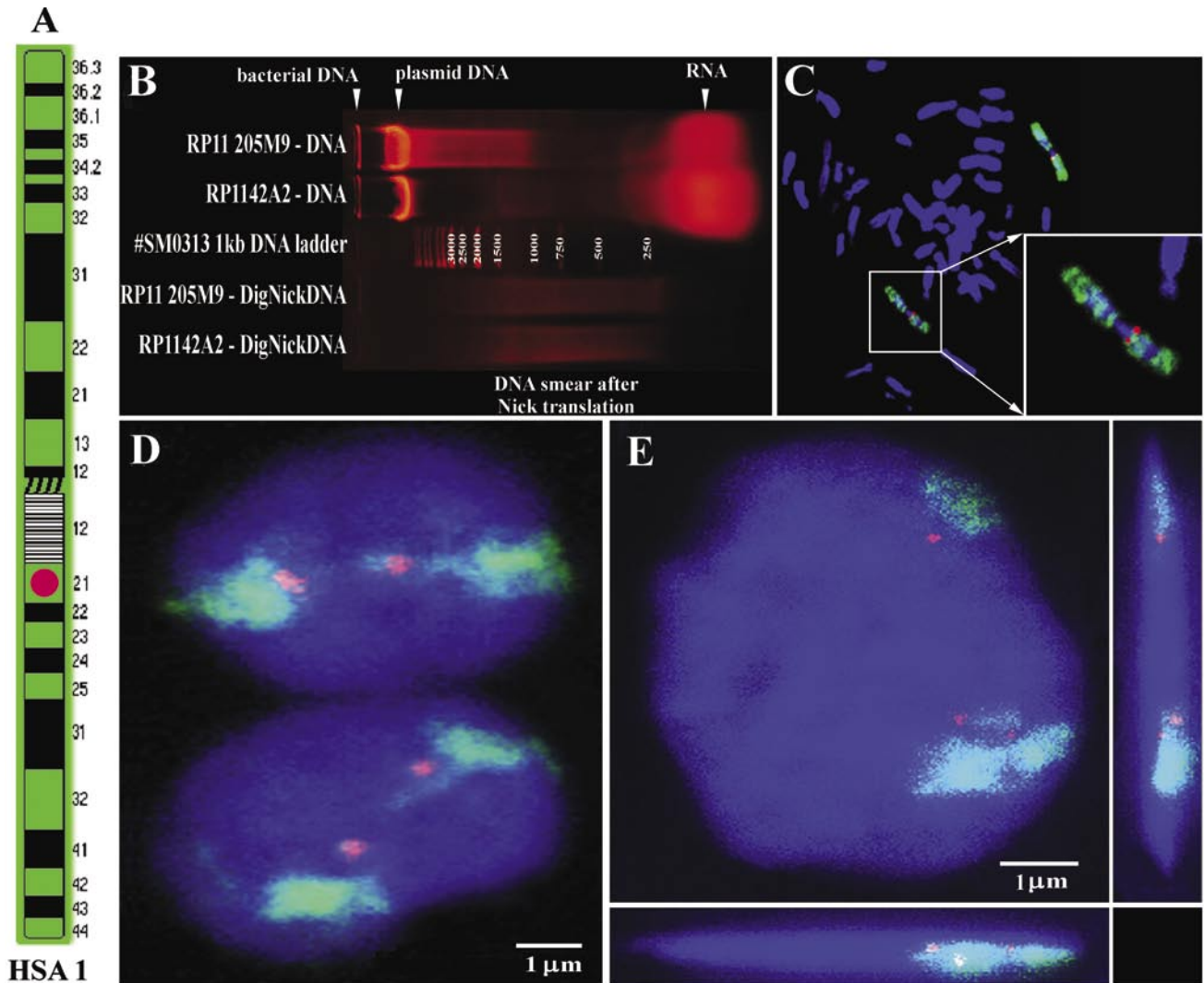


**Figure 1.** A) Mapping of the 1q21 region of human chromosome 1 (HSA 1). B) DNA probe for the 1q21 region was prepared using BAC clones RP11 205M9 and RP1142A2. The purified DNA fragments were labeled using DIG- or Biotin-Nick Translation Mix (Roche, Germany). Every twentieth to twenty-fifth nucleotide was modified with digoxigenin-11-dUTP or biotin-16-dUTP in newly synthesized DNA; the fragment length of the labeled DNA was 200 - 500 bp. C) Stringency of hybridization of the DNA-FISH probe (red) was verified on metaphase spreads in parallel with hybridization of whole chromosome 1 (green). The probe hybridized to the 1q21 region as expected. D) 3D-FISH was performed in order to analyze nuclear distribution of the 1q21 region (red) within the chromosome 1 territory (green) in human peripheral blood lymphocytes. E) 3D-projection of nuclei of ARH-77 cells acquired by Nipkow disc-based confocal microscopy and generated by Andor iQ software. Bars indicate 1  $\mu$ m.

permeabilization solutions. FISH was performed as described in [25, 26, 27, 28]. Detection of HSA1 was carried out using Biotin-Labeled Human Paint Box (Cambio, UK, catalog #1088-B). The genes *c-myc*, *TP53*, *CCND1*, and *IgH* were visualized by the use of PAC clone RP11-968N11 containing the *c-myc* insert and BACs RP11-199F11 (*TP53*), RP11-300I6 (*CCND1*), and RP11-417P24 (*IgH*).

*Cell preparation, fixation and FISH procedures.* In order to verify stringent hybridization of the DNA probes we hybridized probes to metaphase chromosomes (Fig. 1C). Metaphase chromosomes were prepared by standard cytogenetic methods

using colcemid at a final concentration of 0.04  $\mu$ g/ml. Cells were fixed in methanol:acetic acid (3:1), spread onto frozen microscope slides, incubated in  $2\times$  SSC for 30 min at 37°C, and dehydrated by passage through 70%, 80%, and then 100% ethanol. The target DNA was denatured for 2 - 3 min at 72°C in 70% formamide in  $2\times$  SSC, pH 7.0.

We also investigated the location of the 1q21 region within the relevant chromosome 1 (HSA1) territory in interphase nuclei (Fig. 1D). To confirm that hybridization conditions were optimal we carried out confocal microscopy (40 optical sections with an axial step of 0.3  $\mu$ m) and generated 3D-

projections using Andor iQ software (Fig. 1E). To conserve the native three-dimensional structure of interphase nuclei, cells were fixed in 4% formaldehyde. Fixed cells were washed in phosphate-buffered saline (PBS) and treated with 0.02% Triton X-100 for 15 min and then with 0.1 M Tris-Cl, pH 8.0, for 10 min. Cells were permeabilized in 0.1% saponin in PBS for 10 min, washed twice in PBS, and equilibrated for 20 min in 20% glycerol in PBS. The target DNA was denatured for 15 min at 80°C in 50% formamide in PBS. The denatured DNA probe was then applied to the cells and hybridization was performed overnight at 37°C in a humidified chamber. The post-hybridization washing was done according to [29]; briefly, cells were washed in 50% formamide in 2× SSC, pH 7.0, at 43°C for 15 min. The slides were then rinsed in 2× SSC containing 0.1% Tween 20, pH 7.0, at 43°C for 8 min and then in 4× SSC containing 0.2% Igepal at room temperature for 4 min. Rhodamine-antidigoxigenin or FITC-avidin was applied to the slides followed by incubation under a plastic coverslip for 15 min. The coverslip was removed and the slides were washed in 4× SSC containing 0.2% Igepal at 37°C, three times for 4 min each. TO-PRO-3 iodide (Molecular Probes) was used at a concentration of 0.04 µg/ml as a counterstain.

**Image acquisition and statistical evaluation of results.** Image acquisition was carried out by high-resolution cytometry using a Leica DMRXA microscope (Leica, Germany) equipped with a Nipkow disk confocal head [29, 30] and FISH 2.0 software [31]. Forty optical sections with a z-axial step of 0.3 µm were used for 3D-image analysis.

The fluorescence intensity, volume of genetic elements, and the distance of selected genetic elements from the nuclear center were calculated using FISH 2.0 software as described in [31]. Data from FISH 2.0 analysis were exported to Sigma Plot 8.0 software (Jandel Scientific, San Rafael, California, USA) for mathematical evaluation. Statistical analysis was performed using Statistica software (StatSoft CR) and distribution was assessed. The data did not display normal distributions, but were distinctly asymmetric and, therefore, the Mann Whitney (U-test) test was applied to all data.

**Western analysis.** Cell extracts were obtained by lysis in SDS buffer (1 mM Tris, pH 7.5, containing 1% SDS and 20% glycerol). Protein concentration was determined using the DC Protein assay kit (Bio-Rad laboratories, USA). Ten micrograms of total protein from each sample were separated by 10% SDS-PAGE. Proteins were immunodetected using antibodies against PARP (Santa Cruz, USA, catalog no. sc-7150), lamin B (Santa Cruz, USA, catalog no. sc-6217), and Mcl-1 (Santa Cruz, USA, catalog no. sc-819). Western analysis was carried out exactly as described in [32].

## Results

**Nuclear radial distribution of 1q21 region within interphase nuclei of selected cells.** To investigate how gamma-radiation and the cytostatic drugs melphalan and dexamethasone influence the nuclear location of human chromosome 1 (HSA1) and

the 1q21 region we performed analyses in multiple myeloma MOLP-8 cells and lymphoblastoid ARH-77 (Table 1). Similar nuclear parameters were measured in peripheral blood lymphocytes of healthy donors and in the CD138<sup>+</sup> bone marrow fraction of MM patients. We have observed that chromosome 1 and the 1q21 region are positioned more centrally in interphase nuclei of control MOLP-8 cells than in the ARH-77 cell line (Table 1). Only dexamethasone had the effect of changing the nuclear position of the 1q21 region in MOLP-8 cells (Table 1B). The 1q21 region was located more peripherally in interphase nuclei of CD138<sup>+</sup> cells than in peripheral blood lymphocytes, indicating that the chromatin is rearranged in malignant multiple myeloma cells (Table 1C). We also observed an increase in copy number of the 1q21 region in clinical samples; in one sample we identified three copies of 1q21 in 19% of the cells analyzed and four copies in 13% of the cells in another MM patient. The first patient had a normal 1q21 karyotype (Table 1C). An increase in copy number for the 1q21 region was also observed in ARH-77 and MOLP-8 cells (Fig. 2). This was confirmed on metaphase spreads (Fig. 2A and 2D) as well as in interphase nuclei (Fig. 2B, C, E, F) and demonstrating that amplification of 1q21 is a prominent marker of MM cells.

**Nuclear distribution of selected genomic regions in lymphocytes and CD138<sup>+</sup> cells.** In peripheral blood lymphocytes the fluorescence gravity center of HSA1 was located more peripherally than the 1q21 region (Fig. 3A). A similar observation was made in CD138<sup>+</sup> cells of an MM patient (Fig. 3B).

Our structural analyses also investigated the nuclear location of other loci related to MM tumorigenesis and prognosis (Table 2). We observed that in the interphase nuclei of ARH-77 cells only the c-myc gene was located more peripherally than the 1q21 region. CCND1 showed similar nuclear parameters to 1q21, while the TP53 and IgH loci were positioned closer to the nuclear center than 1q21 (Table 1 and Table 2). In MOLP-8 cells c-myc, TP53, CCND1, IgH and the t(CCND1;IgH) translocation were all located more peripherally than the 1q21 region in interphase nuclei. Further, our FISH results confirmed the conclusion drawn from the data in Table 1 that the cytostatic effects of selected clinical agents have a subtle or no influence on cytogenetic parameters such as the nuclear radial distribution of the genetic elements analyzed here.

MOLP-8 cells are characterized by the presence of translocation t(11;14), which involves the CCND1 and IgH loci [33]. Similar to the ARH-77 cells, the c-myc, CCND1, TP53, and IgH loci were not repositioned in interphase nuclei of MOLP-8 cells in response to treatment with cytostatic drugs or gamma-radiation. However, the CCND1/IgH fusion gene (positioned at ~54% of the nuclear radius) was located closer to the fluorescence gravity center than the IgH locus (positioned at ~58% of nuclear radius). The CCND1 locus, which is not involved in the translocation, was also located centrally at 54% of the nuclear radius (Table 2). Cytostatic treatment and gamma-irradiation also did not change the nuclear radial position of fusion genes (Table 2).

**Table 1****A. Average radial distance of HSA1 from the nuclear center (C) in ARH-77 and MOLP-8 cells.**

ARH-77	C-HSA 1/R ± S.E. (%)	MOLP-8	C-HSA 1/R ± S.E. (%)
control	66.0 ± 2.7	control	60.5 ± 1.9
melphalan	68.1 ± 3.2	melphalan	58.3 ± 2.1
dexamethasone	69.2 ± 4.4	dexamethasone	61.7 ± 2.0
γ-irradiation	62.6 ± 2.0	γ-irradiation	64.5 ± 3.3

**B. Average radial distance of the 1q21 region from the nuclear center (C) in ARH-77 and MOLP-8 cells**

ARH-77	C-1q21/R ± S.E. (%)	MOLP-8	C-1q21/R ± S.E. (%)
control	60.2 ± 2.3	control	48.8 ± 2.0
melphalan	64.0 ± 2.9	melphalan	57.3 ± 2.8
dexamethasone	59.7 ± 1.9	dexamethasone	60.8 ± 2.7 *
γ-irradiation	63.2 ± 1.7	γ-irradiation	56.6 ± 3.6

Asterisk (\*) indicates P ≤ 005.

**C. Average radial distance of the 1q21 region from the nuclear center (C) in lymphocytes and CD138<sup>+</sup> multiple myeloma cells.**

	Signals (No.)	Cells (%)	C-1q21/R ± S.E. (%)	R ± S.E. (μm)
<b>Lymphocytes</b>	2	100	43.4 ± 0.7	1.9 ± 0.1
<b>CD 138<sup>+</sup> MM cells</b>	patient 1	68	48.9 ± 0.9 *	
	patient 2	19	57.1 ± 3.4 *	2.2 ± 0.1
	patient 3	13	57.5 ± 4.3 *	

Asterisk (\*) indicates P ≤ 005. R represents average radius of nuclei. All data are normalized to the local nuclear radius (R).

**Table 2. Average radial distance between selected genes and the nuclear center in ARH-77 and MOLP-8 cells.**

ARH-77	C-c-myc/R ± S.E. (%)	C-TP53/R ± S.E. (%)	C-CCND1/R ± S.E. (%)	C-IgH/R ± S.E. (%)
No. of signals analyzed	5	2	3	3
control	65.1 ± 1.2	52.0 ± 1.3	60.0 ± 1.6	55.5 ± 1.5
dexamethasone	64.0 ± 1.9	49.3 ± 0.5	58.1 ± 1.4	55.3 ± 1.3
melphalan	61.3 ± 1.6	50.5 ± 0.6	59.2 ± 1.2	56.1 ± 1.3
γ-irradiation	64.0 ± 1.8	49.3 ± 0.5	55.4 ± 1.1	60.4 ± 1.1

MOLP-8 (signal no.)	C-c-myc/R ± S.E. (%)	C-TP53/R ± S.E. (%)	C-CCND1/R ± S.E. (%)	C-IgH/R ± S.E. (%)	C-t(CCND1/IgH) /R ± S.E. (%)
No. of signals analyzed	3	2	1#	3	1
control	63.4 ± 1.5	51.7 ± 1.6	53.6 ± 1.3	57.9 ± 1.1	53.5 ± 1.5
dexamethasone	65.1 ± 1.3	47.6 ± 1.5	60.1 ± 2.5	60.8 ± 2.6	55.6 ± 2.4
melphalan	64.4 ± 1.2	51.2 ± 1.0	51.2 ± 1.7	55.3 ± 1.7	52.7 ± 1.3
γ-irradiation	64.4 ± 1.3	51.6 ± 1.3	52.5 ± 1.7	56.7 ± 1.7	54.3 ± 1.4

Data are expressed as percentages and are normalized to the local nuclear radius (R). All measurements were performed 24 hours after cytostatic treatment. Clinically used cytostatic agents and gamma-radiation have no effect on nuclear parameters such as the number of numerical aberrations and the distance between the fluorescence gravity centers of nuclei and selected genes.

#, a second signal was involved in translocation.

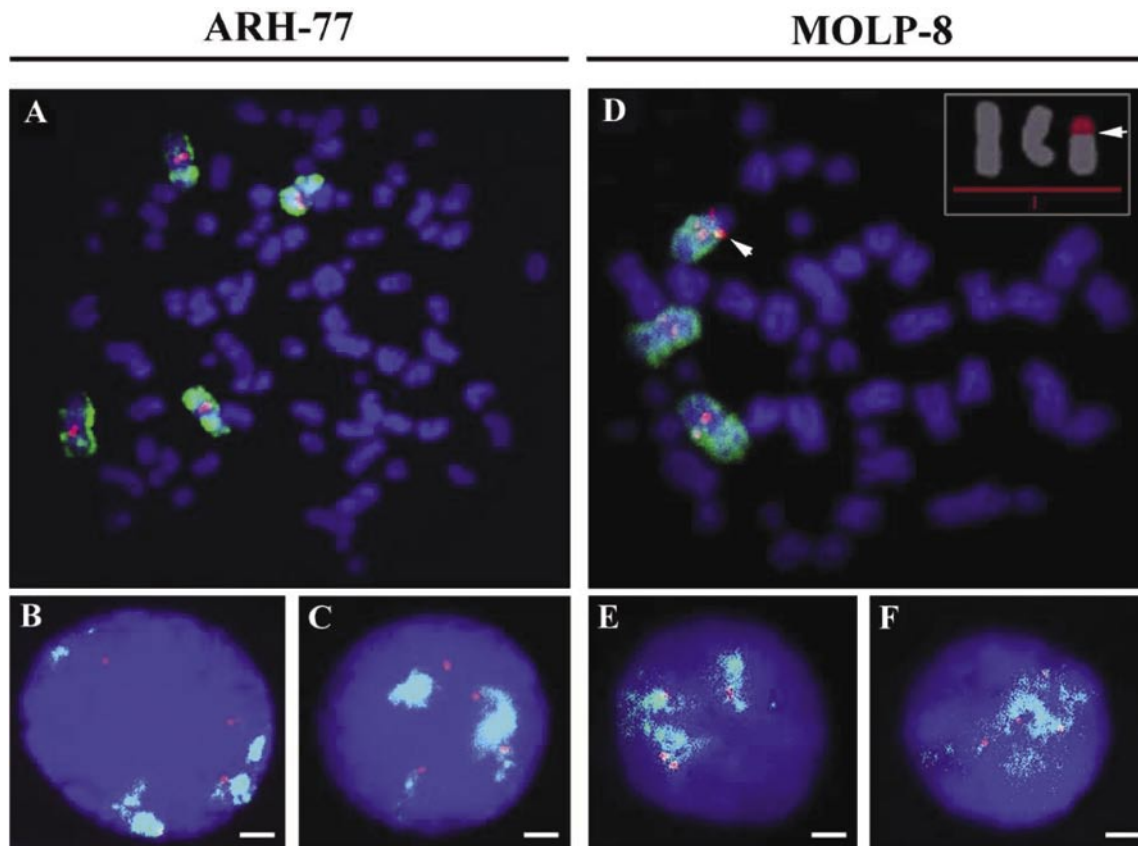


**Figure 2.** A) Analysis of the 1q21 region (red) of HSA1 (green) in mitotic chromosomes of ARH-77 cells and B and C) in interphase nuclei of ARH-77 cells. D) The 1q21 region (red) and HSA1 (green) in mitotic chromosomes of MOLP-8 cells and E and F) in interphase nuclei of MOLP-8 cells. Bars indicate 0.5  $\mu\text{m}$ .

*Mcl-1* gene, mapped to 1q21 region, is an important diagnostic marker for MM. Mcl-1 is an anti-apoptotic Bcl-2 family protein and has been identified as an important factor in early induction during myeloblastic leukemia cell differentiation [21]. Mcl-1 can be alternatively spliced into long (Mcl-1<sub>L</sub>) and short (Mcl-1<sub>S</sub>) variants. The role of this protein is discussed with respect to multiple myeloma in [22]. In our study western analysis of the long (Mcl-1<sub>L</sub>) and short (Mcl-1<sub>S</sub>) forms showed that only MM MOLP-8 cells express the short Mcl-1<sub>S</sub> variant at high levels, suggesting that this variant may be an important marker that could be used in MM diagnosis. The Mcl-1<sub>L</sub> form was expressed in both lymphoblastoid and myeloma cells, but the highest level was again observed in the MOLP-8 cells. Both ARH-77 and MOLP-8 cells express a significantly higher level of Mcl-1<sub>L</sub> than peripheral blood lymphocytes and variant Mcl-1<sub>S</sub> is completely absent in lymphocytes of healthy donors (Fig. 4). Because Mcl-1 is associated with induction of apoptosis, we also analyzed the other markers of this type of cell death, PARP (120 kDa) and lamin B (60 kDa). Using western analysis we examined the levels of the 80-kDa PARP cleavage product,

an indicator of the presence of apoptotic cells, and observed that melphalan and gamma-irradiation are strong inducers of apoptosis in both ARH-77 and MOLP-8 cells. In contrast, dexamethasone treatment increased PARP cleavage to a level only slightly above background (Fig. 4). Similarly, cleavage of lamin B (60 kDa) into a 45-kDa fragment was significantly increased after melphalan treatment and gamma-irradiation (Fig. 4).

### Discussion

In this study we have presented an analysis of the nuclear radial distribution of the 1q21 region, which is an important diagnostic and prognostic tool for multiple myeloma. In addition, we have shown that the Mcl-1 gene, which maps to the 1q21 region, and its protein variants (Mcl-1<sub>L</sub>) and (Mcl-1<sub>S</sub>) can serve as valuable diagnostic tools for clinics dealing with MM pathophysiology.

When we analyzed the nuclear radial distribution of HSA1 and its 1q21 region and the *c-myc*, *CCND1*, *TP53*, and *IgH*

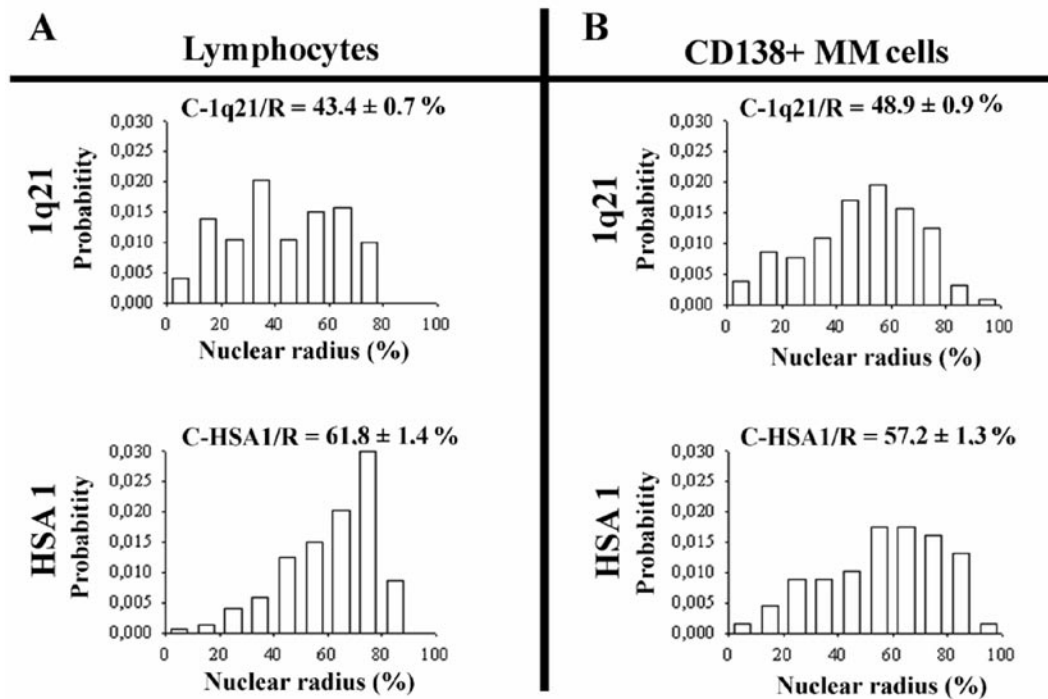


Figure 3. A) Nuclear radial distribution of the 1q21 region and HSA 1 in peripheral blood lymphocytes and B) in CD138<sup>+</sup> bone marrow cells isolated from MM patients. Average values ± S.E. are shown as a percent of the nuclear radius (R). Approximately 200 nuclei were evaluated in each of two independent experiments.

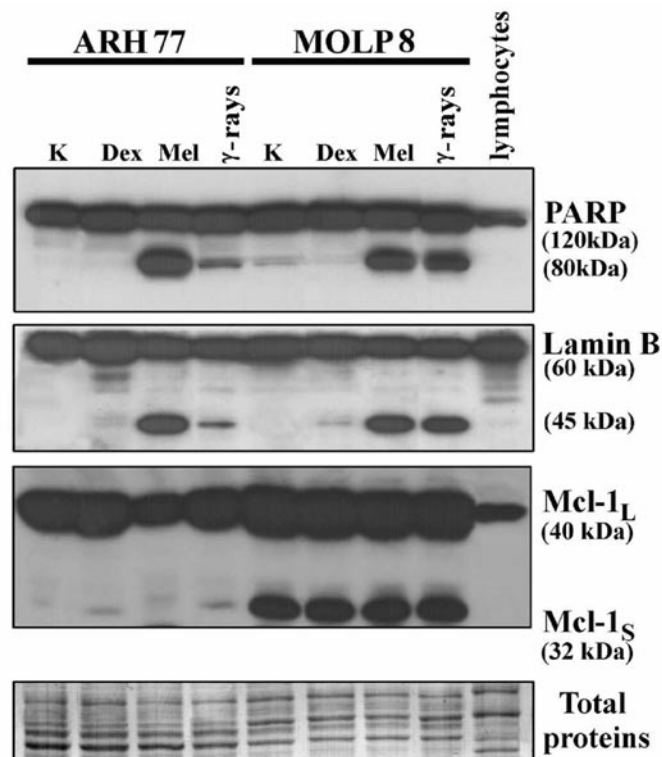


Figure 4. Western analysis of PARP, lamin B, and Mcl-1 variants. Evidence of apoptotic cleavage of PARP (120 kDa) into an 80-kDa fragment and of lamin B (60 kDa) into a 45-kDa fragment was observed. The full-length large Mcl-1<sub>L</sub> (40 kDa) and short Mcl-1<sub>S</sub> (32 kDa) variants were examined in control, dexamethasone- and melphalan-treated, and gamma-irradiated ARH-77 and MOLP-8 cells. Levels of all proteins were related to the equal total protein levels, as shown in the bottom panel.

genes in either lymphoblastoid ARH-77 or MOLP-8 MM cells that had been treated with clinically-used cytostatic drugs or gamma-radiation, in the majority of cases we observed no significant changes in nuclear radial positioning (Table 1 and Table 2). Unchanged nuclear arrangement after gamma-radiation is also documented by Jirsova [34], where altered loci positions were reported within a short time (2h) of gamma-radiation. However, the loci were restored to their original nuclear positions with prolonged 24h-cell cultivation after irradiation. The relatively conserved nuclear locations of the TP53 and RB1 genes after gamma-radiation were also observed in our previous studies with retinoblastoma cells; however, cisplatin treatment resulted in repositioning of TP53 and Rb1 closer to the nuclear center [26]. This implies that different cytostatic drugs have distinct effects on the nuclear radial arrangement of tumor suppressor genes and, importantly, that these effects are cell-type-dependent.

The next part of our analysis of nuclear radial arrangements addressed the derivative chromosome, which results from the translocation of the CCND1 and IgH genes in MOLP-8 MM cells. We observed that the fusion gene was positioned at approximately 54% of the nuclear radius, similar to the karyotypically normal CCND1 gene (Table 2). In contrast, the IgH gene was located at approximately 58% of the nuclear radius in control and cytostatic-treated MOLP-8 cells (Table 2B). This observation was reproduced in all cases studied. The central nuclear positioning of the normal CCND1 gene in MOLP-8 cells (Table 2B) is probably associated with the increased transcriptional activity of CCND1 in these cells [35]. This observation correlates well with the widely-observed phenomenon that sites of active transcription are preferentially located in the nuclear interior [30, 36, 37], while silenced loci occupy the more peripheral regions of interphase nuclei [38]. Surprisingly, our structural data on the nuclear radial distribution of translocated loci do not correlate with previously data reported [27, 28], suggesting that the average nuclear radial positions of fusion genes are determined by the final structure of the derivative chromosome on which they are located. Similarly, in a patient suffering from chronic myeloid leukemia, the BCR/ABL fusion gene was positioned at an intermediate distance from the normal BCR and ABL genes in leukemia cells [32]. These contradictions can be explained by the appearance of an additional t(4;11) translocation involving the CCND1 gene in MOLP-8 cells [33]. This chromosomal rearrangement could influence the nuclear radial distribution of other CCND1 loci not involved in t(11;14). Nevertheless, all these data support the conclusion that disorder in spatial genome organization increases the probability of inducing chromosome translocations as reported by Kozoubek and Roix [39, 40] and summarized by Soutoglou [41]. Kozubek et al. [39] have shown that the physical distance between loci is an important parameter for the induction of nuclear processes that lead to structural aberrations such as translocations. Moreover, as suggested by Meaburn [42], knowledge of the precise functional relevance of gene positioning in cancer cells could influence the direction and suggest new strategies for early cancer diagnosis.

Similarly, a regulatory function of the Mcl-1 protein, particularly its truncated variant Mcl-1<sub>s</sub>, represents an attractive target for future MM therapeutic interventions. The Mcl-1<sub>s</sub> variant may be not only a promising diagnostic tool for MM, but may also serve as a specific target for anticancer therapy.

**Acknowledgement.** This work was supported by The Ministry of Education, Youth, and Sports of the Czech Republic, Grant No. LC06027, and the following projects: AVOZ50040507, AVOZ50040702, and IQS500040508.

## References

- [1] PRATT G. Molecular aspects of multiple myeloma. *Mol Pathol.* 2002; 55: 273–283. Review. doi:10.1136/mp.55.5.273 PMID:12354927 PMCID:1187254
- [2] FONSECA R, BAILEY RJ, AHMANN GJ, et al. Genomic abnormalities in monoclonal gammopathy of undetermined significance. *Blood.* 2002; 100: 1417–1424.
- [3] SMADJA NV, BASTARD C, BRIGAUDEAU C et al., Groupe Français de Cytogénétique Hématologique. Hypodiploidy is a major prognostic factor in multiple myeloma. *Blood.* 2001; 98: 2229–2238. doi:10.1182/blood.V98.7.2229 PMID:11568011
- [4] KUEHL WM, BERGSAGEL PL. Multiple myeloma: evolving genetic events and host interactions. *Nat Rev Cancer.* 2002; 2: 175–187. doi:10.1038/nrc746 PMID:11990854
- [5] CREMER FW, BILA J, BUCK I, et al. Delineation of distinct subgroups of multiple myeloma and a model for clonal evolution based on interphase cytogenetics. *Genes Chromosomes Cancer.* 2005(a); 44: 194–203.
- [6] SHAUGHNESSY J, TIAN E, SAWYER J, et al. High incidence of chromosome 13 deletion in multiple myeloma detected by multiprobe interphase FISH. *Blood.* 2000; 96: 1505–1511.
- [7] CREMER FW, KARTAL M, HOSE D, et al. High incidence and intraclonal heterogeneity of chromosome 11 aberrations in patients with newly diagnosed multiple myeloma detected by multiprobe interphase FISH. *Cancer Genet Cytogenet.* 2005(b); 161: 116–124.
- [8] AVET-LOISEAU H, GERSON F, MAGRANGEAS F, et al. Intergroupe Francophone du Myelome. Rearrangements of the c-myc oncogene are present in 15% of primary human multiple myeloma tumors. *Blood.* 2001; 98: 3082–3086. doi:10.1182/blood.V98.10.3082 PMID:11698294
- [9] LIU P, LEONG T, QUAM L, et al. Activating mutations of N- and K-ras in multiple myeloma show different clinical associations: analysis of the Eastern Cooperative Oncology Group Phase III Trial. *Blood.* 1996; 88: 2699–2706.
- [10] HAROUSSEAU JL, SHAUGHNESSY JR, RICHARDSON P. Multiple myeloma. *Hematology Am Soc Hematol Educ Program.* 2004; 237–256. doi:10.1182/asheducation-2004.1.237
- [11] KUDOH K, KIKUCHI Y, KITA T et al. Preoperative determination of several serum tumor markers in patients with primary epithelial ovarian carcinoma. *Gynecol Obstet Invest.* 1999; 47: 52–57. doi:10.1159/000010062 PMID:9852392
- [12] TARKKANEN M, HUUHTANEN R, VIROLAINEN M. et al. Comparison of genetic changes in primary sarcomas and their pulmonary metastases. *Genes Chromosome Cancer.* 1999;

- 25: 323–31. doi:10.1002/(SICI)1098-2264(199908)25:4<323::AID-GCC3>3.0.CO;2-5 PMID:10398425
- [13] PETERSEN I, HIDALGO A, PETERSEN S, et al. Chromosomal imbalances in brain metastases of solid tumors. *Brain Pathol.* 2000; 10: 395–401.
- [14] ITOYAMA T, NANJUGUD G, CHEN W, et al. Molecular cytogenetic analysis of genomic instability at the 1q12-22 chromosomal site in B-cell non-Hodkin lymphoma. *Genes Chromosomes Cancer.* 2002; 35: 318–28. doi:10.1002/gcc.10120 PMID:12378526
- [15] HANAMURA I, STEWART JP, HUANG Y, et al. Frequent gain of chromosome band 1q21 in plasma-cell dyscrasias detected by fluorescence in situ hybridization: incidence increases from MGUS to relapsed myeloma and is related to prognosis and disease progression following tandem stem-cell transplantation. *Blood.* 2006; 108: 1724–1732. doi:10.1182/blood-2006-03-009910 PMID:16705089 PMCid:1895503
- [16] SONNEVELD P. Gain of 1q21 in multiple myeloma from bad to worse. *Blood.* 2006; 108: 1426–1427. doi:10.1182/blood-2006-06-028530
- [17] WALKER, BA, LEONE, PE, JENNER, MW, et al. Integration of global SNP-based mapping and expression arrays reveals key regions, mechanisms, and genes important in the pathogenesis of multiple myeloma. *Blood* 2006; 108: 1733–1734. doi:10.1182/blood-2006-02-005496 PMID:16705090
- [18] SHAUGHNESSY J. Amplification and overexpression of CDK1B at chromosome band 1q21 is associated with reduced levels of p27Kip1 and an aggressive clinical course in multiple myeloma. *Hematology.* 2005; 10: 117–126. doi:10.1080/10245330512331390140 PMID:16188652
- [19] DREWINKO B, MARS W, MINOWADA J, et al. ARH-77, an established human IgG-producing myeloma cell line. I. Morphology, B-cell phenotypic marker profile, and expression of Epstein-Barr virus. *Cancer.* 1984(a); 54: 1883–1892.
- [20] DREWINKO B, MARS W, STRAGAND JJ, et al. ARH-77, an established human IgG-producing myeloma cell line. II. Growth kinetics, clonogenic capacity, chalone production, xenogeneic transplantations, and response to melphalan. *Cancer.* 1984(b); 54: 1893–1903.
- [21] BAE J, LEO CP, HSU SY, et al. MCL-1S, a Splicing variant of the antiapoptotic Bcl-2 member MCL-1, encodes a proapoptotic protein possessing only the BH3 domain. *J Biol Chem.* 2000; 275: 25255–25261. doi:10.1074/jbc.M909826199 PMID:10837489
- [22] LE GOUILL S, PODAR K, HAROUSSEAU JL et al. Mcl-1 regulation and its role in multiple myeloma. *Cell Cycle.* 2004; 3: e107–e110.
- [23] FIŠEROVÁ A, HÁJEK R, HOLUBOVÁ V, et al. Detection of 13q abnormalities in multiple myeloma using immunomagnetically selected plasma cells. *Neoplasma.* 2002; 49: 300–306.
- [24] BÁRTOVÁ E, KOZUBEK S, JIRSOVÁ P, et al. Higher-order chromatin structure of human granulocytes. *Chromosoma.* 2001; 110: 360–370. doi:10.1007/s004120100141 PMID:11685536
- [25] BÁRTOVÁ E, KOZUBEK S, KOZUBEK M, et al. The influence of the cell cycle, differentiation and irradiation on the nuclear location of the abl, bcr and c-myc genes in human leukemic cells. *Leuk Res.* 2000; 24: 233–241. doi:10.1016/S0145-2126(99)00174-5 PMID:10739005
- [26] BÁRTOVÁ E, KOZUBEK S, GAJOVÁ H et al. Cytogenetics and cytology of retinoblastomas. *J Cancer Res Clin Oncol.* 2003; 129: 89–99.
- [27] TASLEROVÁ R, KOZUBEK S, LUKÁŠOVÁ E et al. Arrangement of chromosome 11 and 22 territories, EWSR1 and FLI1 genes, and other genetic elements of these chromosomes in human lymphocytes and Ewing sarcoma cells. *Hum Genet.* 2003; 112: 143–155.
- [28] TASLEROVÁ R, KOZUBEK S, BÁRTOVÁ E et al. Localization of genetic elements of intact and derivative chromosome 11 and 22 territories in nuclei of Ewing sarcoma cells. *J Struct Biol.* 2006; 155: 493–504. doi:10.1016/j.jsb.2006.05.005 PMID:16837212
- [29] KREJČÍ J, HARNIČAROVÁ A, KŮROVÁ J et al. Nuclear organization of PML bodies in leukaemic and multiple myeloma cells. *Leuk Res.* 2008; 32: 1866–1877. doi:10.1016/j.leukres.2008.04.021 PMID:18534676
- [30] HARNIČAROVÁ A, KOZUBEK S, PACHERNÍK J et al. Distinct nuclear arrangement of active and inactive c-myc genes in control and differentiated colon carcinoma cells. *Exp Cell Res.* 2006; 312: 4019–4035. doi:10.1016/j.yexcr.2006.09.007 PMID:17046748
- [31] KOZUBEK M, KOZUBEK S, LUKÁŠOVÁ E, et al. High-resolution cytometry of FISH dots in interphase cell nuclei. *Cytometry.* 1999; 36: 279–293. doi:10.1002/(SICI)1097-0320(19990801)36:4<279::AID-CYTO2>3.0.CO;2-G PMID:10404143
- [32] BÁRTOVÁ E, HARNIČAROVÁ A, PACHERNÍK J, et al. Nuclear topography and expression of the BCR/ABL fusion gene and its protein level influenced by cell differentiation and RNA interference. *Leuk Res.* 2005; 29: 901–913. doi:10.1016/j.leukres.2005.01.011 PMID:15978941
- [33] MATSUO Y, DREXLER HG, HARASHIMA A, et al. Induction of CD28 on the new myeloma cell line MOLP-8 with t(11;14)(q13;q32) expressing delta/lambda type immunoglobulin. *Leuk Res.* 2004; 28: 869–877. doi:10.1016/j.leukres.2003.12.008 PMID:15203285
- [34] JIRSOVÁ P, KOZUBEK S, BÁRTOVÁ E, et al. Spatial distribution of selected genetic loci in nuclei of human leukemia cells after irradiation. *Radiat Res.* 2001; 155: 311–319. doi:10.1667/0033-7587(2001)155[0311:SDOSGL]2.0.CO;2 PMID:11175666
- [35] PRUNERI G, FABRIS S, BALDINI L, et al. Immunohistochemical analysis of cyclin D1 shows deregulated expression in multiple myeloma with the t(11;14). *Am J Pathol.* 2000; 156: 1505–1513.
- [36] WILLIAMS RR, AZUARA V, PERRY P, et al. Neural induction promotes large-scale chromatin reorganisation of the Mash1 locus. *J Cell Sci.* 2006; 119: 132–140. doi:10.1242/jcs.02727 PMID:16371653
- [37] ZINK D, AMARAL MD, ENGLMANN A, et al. Transcription-dependent spatial arrangements of CFTR and adjacent genes in human cell nuclei. *J Cell Biol.* 2004; 166: 815–825. doi:10.1083/jcb.200404107 PMID:15364959 PMCid:2172106
- [37] BÁRTOVÁ E, KOZUBEK S. Nuclear architecture in the light of gene expression and cell differentiation studies. *Biol Cell* 2006; 98: 323–336. doi:10.1042/BC20050099 PMID:16704376

- [39] KOZUBEK S, LUKÁŠOVÁ E, RÝZNAR L, et al. Distribution of ABL and BCR genes in cell nuclei of normal and irradiated lymphocytes. *Blood*. 1997; 89: 4537–4545.
- [40] ROIX JJ, MCQUEEN PG, MUNSON PJ et al. Spacial proximity of translocation-prone gene loci in human lymphomas. *Nat Genet*. 2003; 34: 287–291. [doi:10.1038/ng1177](https://doi.org/10.1038/ng1177) PMID:12808455
- [41] SOUTOGLOU E, MISTELI T. Mobility and immobility of chromatin in transcription and genome stability. *Curr Opin Genet Dev*. 2007; 17: 435–42. Epub 2007 Oct 1. Review. [doi:10.1016/j.gde.2007.08.004](https://doi.org/10.1016/j.gde.2007.08.004) PMID:2118061
- [42] MEABURN KJ, MISTELI T. Locus-specific and activity-independent gene repositioning during early tumorigenesis. *J Cell Biol*. 2008; 180: 39–50. [doi:10.1083/jcb.200708204](https://doi.org/10.1083/jcb.200708204) PMID:18195100 PMID:2213600